Cell Metabolism, Volume *33*

Supplemental information

Obesity-associated hyperleptinemia alters the gliovascular interface of the hypothalamus to promote hypertension

Tim Gruber, Chenchen Pan, Raian E. Contreras, Tobias Wiedemann, Donald A. Morgan, Alicja A. Skowronski, Sandrine Lefort, Cahuê De Bernardis Murat, Ophelia Le Thuc, Beata Legutko, Francisco J. Ruiz-Ojeda, María de la Fuente-Fernández, Angel Luis García-Villalón, Daniel González-Hedström, Melanie Huber, Klara Szigeti-Buck, Timo D. Müller, Siegfried Ussar, Paul Pfluger, Steve C. Woods, Ali Ertürk, Charles A. LeDuc, Kamal Rahmouni, Miriam Granado, Tamas L. Horvath, Matthias H. Tschöp, and Cristina García-Cáceres

Cell Metabolism, Volume *33*

Supplemental information

Obesity-associated hyperleptinemia alters the gliovascular interface of the hypothalamus to promote hypertension

Tim Gruber, Chenchen Pan, Raian E. Contreras, Tobias Wiedemann, Donald A. Morgan, Alicja A. Skowronski, Sandrine Lefort, Cahuê De Bernardis Murat, Ophelia Le Thuc, Beata Legutko, Francisco J. Ruiz-Ojeda, María de la Fuente-Fernández, Angel Luis García-Villalón, Daniel González-Hedström, Melanie Huber, Klara Szigeti-Buck, Timo D. Müller, Siegfried Ussar, Paul Pfluger, Steve C. Woods, Ali Ertürk, Charles A. LeDuc, Kamal Rahmouni, Miriam Granado, Tamas L. Horvath, Matthias H. Tschöp, and Cristina García-Cáceres

Supplemental items

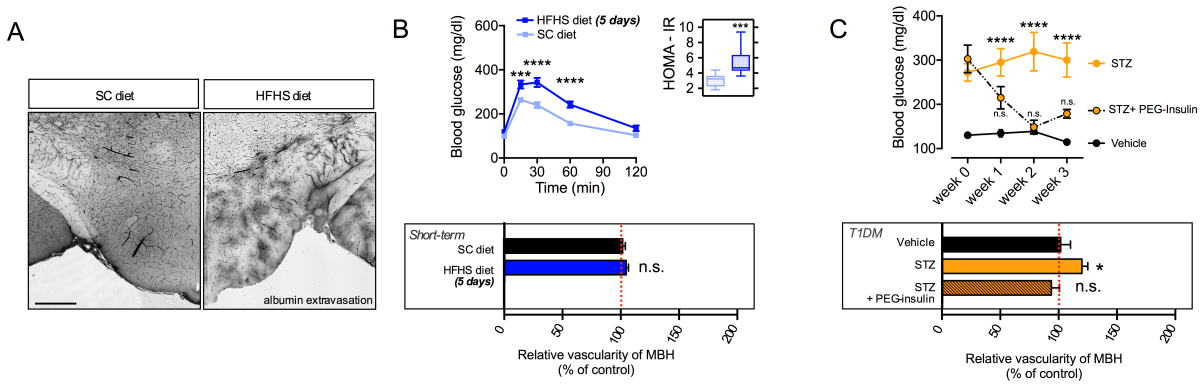

Figure S1. Related to Figure 1: Impaired glucose metabolism does not underlie the dynamic remodelling of the hypothalamic vasculature.

(A) Overview confocal micrograph of albumin extravasation in C57BL/6J mice exposed to SC or HFHS diet. Scale bar, 500 µm.

(B) Blood glucose traces upon an intraperitoneal glucose tolerance test (2 g/kg BW glucose; *i.p.*) in C57BL/6J mice fed SC diet or 5-days HFHS diet (top left panel) and calculated HOMA-IR (top right panel); quantification of MBH vascularity in SC diet and 5-days HFHS diet-fed mice relative to SC diet control group. Data are presented as mean ± SEM. *** $P < 0.001$, **** $P < 0.0001$, n.s., not significant. n = 10-12 mice (two-way ANOVA and unpaired Student's *t*-test).

(C) Weekly *ad-libitum* blood glucose levels in C57BL/6J mice that received either STZ (50 mg/kg BW, *i.p.* over initial 5 days), STZ (50 mg/kg BW, *i.p.* over initial 5 days) + PEG-insulin (25 nmol/kg BW/day following STZ) or vehicle; quantification of MBH vascularity in STZ-treated, STZ + PEG-insulin-treated, and vehicle treated mice relative to vehicle-treated control mice. Diet and 5-days HFHS diet-fed mice relative to SC diet control group. Data are presented as mean ± SEM. *** $P < 0.001$, **** $P < 0.0001$, n.s., not significant. n = 6 mice (one-way ANOVA and two-way ANOVA).

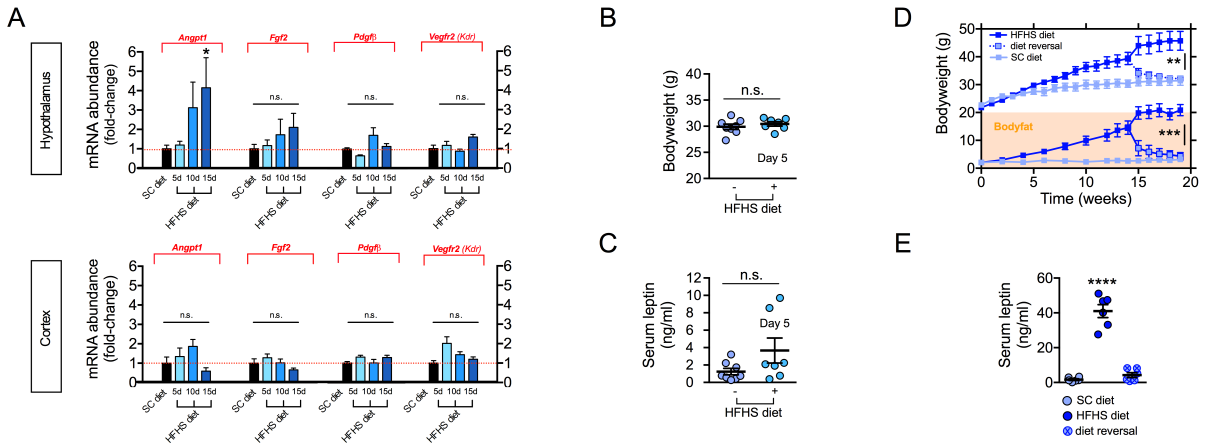

Figure S2. Related to Figure 2: Time-course expression screen of HFHS diet-induced, pro-angiogenic factors in the mouse brain as well as bodyweight and serum leptin upon short- and long-term HFHS diet exposure.

(A) qPCR analysis of pro-angiogenic genes angiopoietin 1 (*Angpt1*), fibroblast growth factor 2 (*Fgf2*), platelet-derived growth factor *β (Pdgfβ*), vascular endothelial growth factor 2/kinase insert domain receptor (*Vegfr2/Kdr*) in the hypothalamus (top panel) and cortex (lower panel) of C57BL/6J mice exposed to HFHS diet for 5, 10 or 15 days normalized to SC-fed controls. Data are presented as mean ± SEM. * $P < 0.05$, n.s., not significant. n = 8 mice (one-way ANOVA).

(B) Bodyweight of C57BL/6J mice exposed to 5 days HFHS diet versus SC diet. Data are presented as mean ± SEM. n.s., not significant. n = 7-8 mice (unpaired Student's *t*-test).

(C) Serum leptin levels of C57BL/6J mice exposed to 5 days HFHS diet versus SC diet. Data are presented as mean ± SEM. n.s., not significant. n = 7-8 mice (unpaired Student's *t*-test).

(D) Bodyweight and body fat trajectory of C57BL/6J mice fed SC diet (20 weeks), HFHS diet (20 weeks) or HFHS diet (15weeks) + reversal to SC diet (5 weeks). Data are presented as mean ± SEM. ** $P < 0.01$, *** $P < 0.001$. n = 4 mice (two-way ANOVA).

(E) Serum leptin levels of C57BL/6J mice fed SC diet (20 weeks), HFHS diet (20 weeks) or HFHS diet (15weeks) + reversal to SC diet (5 weeks). Data are presented as mean ± SEM. **** $P < 0.0001$. n = 6 mice (one-way ANOVA).

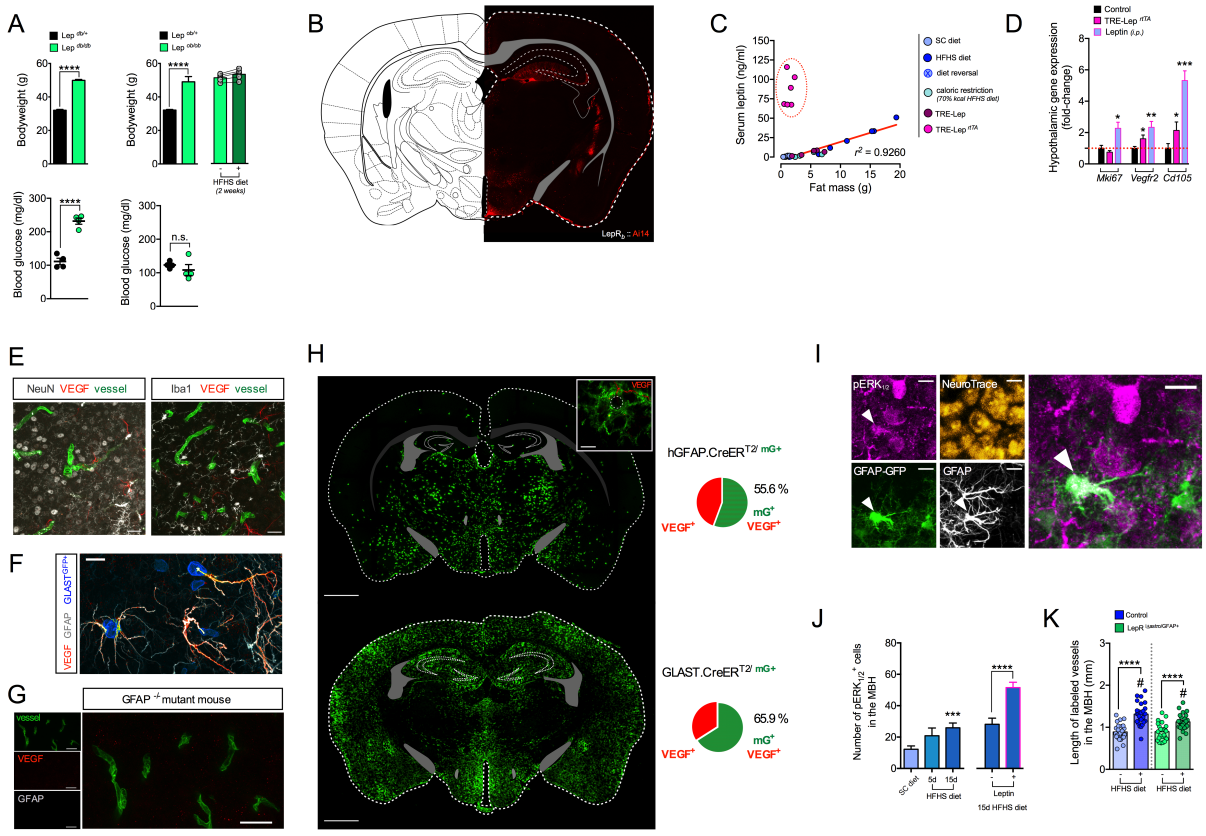

Figure S3. Related to Figure 3: Bodyweight changes in Lep$^{ob/ob}$ mice upon leptin substitution and the characterization of astrocyte-specific Cre-driver mouse models to target astroglial VEGF.

(A) Bodyweight and glycemia of leptin receptor-deficient Lep$^{db/db}$ and heterozygous Lep$^{db/+}$ control mice fed SC diet (left panel) as well as of SC diet-fed leptin-deficient Lep$^{ob/ob}$ and heterozygous Lep$^{ob/+}$ control mice (right) including bodyweight change of a sub-cohort of Lep$^{ob/ob}$ mice exposed to HFHS (2 weeks). Data are presented as mean ± SEM. **** $P < 0.0001$. n = 4 mice (unpaired Student's *t*-test).

(B) Schematic coronal diagram (Allen brain atlas) next to a confocal micrograph of LepRb:Ai14 reporter mouse.

(C) Linear regression analysis of serum leptin levels and body fat across C57BL/6J mice fed SC diet, HFHS diet, diet reversal (HFHS > SC diet), calorie restriction (70 % of HFHS diet *ad libitum* intake) and TRE-Lep and TRE-Lep^{rtTA} mice (doxycycline supplemented drinking water for 4 weeks); discordance of serum leptin and adiposity is highlighted for lean but hyperleptinemic TRE-Lep^{rtTA} mice (red circle).

(D) Hypothalamic gene expression of marker of proliferation Ki67 (*Mki67*), vascular endothelial growth factor 2/kinase insert domain receptor (*Vegfr2/Kdr*) and cluster of differentiation 105 (*Cd105/endoglin*) as markers of endothelial proliferation in C57BL/6J mice fed SC diet treated with

leptin (3 mg/kg BW; *i.p.* twice a day for 3 days; see Figure 3B) and TRE-Lep^{rtTA} mice (doxycycline supplemented drinking water for 4 weeks) relative to respective controls. Data are presented as mean ± SEM. * P < 0.05, ** P < 0.01, *** P < 0.001. n = 8-12 mice (one-way ANOVA).

(E) Confocal micrographs showing the absence of VEGF immunoreactivity (red) in neurons (NeuN^{+}; gray) and microglia (Iba1^{+}; gray) along with the microvasculature (green) in the mediobasal hypothalamus (MBH) of C57BL/J6 exposed to a HFHS diet. Scale bar, 10 µm.

(F) Exemplary confocal micrograph showing hypothalamic VEGF immunoreactivity (red) colocalizing with either GFAP-immunoreactive filaments (gray), GLAST.CreER^{T2+} astrocytes tagged with tamoxifen-inducible nuclear GFP (blue), or both. Scale bar, 10 µm.

(G) Confocal micrograph of hypothalamic VEGF (red) and GFAP (gray) immunoreactivity along with the microvasculature (green) of a global GFAP$^{-/-}$ mutant mouse. Scale bar, 25 µm.

(H) Confocal micrographs of coronal brain sections of hGFAP.CreER$^{T2/mG+}$ (upper panel) and GLAST.CreER$^{T2/mG+}$ (lower panel) demonstrate characteristic Cre-recombination patterns of respective astrocyte-specific Cre-driver lines throughout the brain (mG^{+}; green); illustrative high-magnification insert depicting an individual hypothalamic hGFAP.CreER$^{T2/mG+}$ astrocyte (green) exhibiting VEGF immunoreactivity (red). Pie chart analysis demonstrating the fraction of VEGF^{+} astrocytes in the hypothalamus targeted by Cre-mediated recombination in hGFAP.CreER$^{T2/mG+}$ and GLAST.CreER$^{T2/mG+}$, respectively. n = 3 mice.

(I) Representative high-magnification confocal scans of phosphorylated extracellular regulated kinase ½ (pERK$_{1/2}$) immunoreactivity colocalizing with neurons (NeuroTrace; yellow) but also astrocytes as identified by both AAV2/5Gfa2.GFP (GFAP-GFP; green) and GFAP immunoreactivity (grey). Scale bar, 10 µm.

(J) Quantification of pERK$_{1/2}$-immunoreactive cells in the MBH of male C57BL/6J mice fed SC diet, 5 or 15 days HFHS diet or 15 days HFHS diet with additional injection of leptin (5 mg/kg BW; *i.p.*) *versus* vehicle. Data are presented as mean ± SEM. *** P < 0.001 (one-way ANOVA), **** P < 0.0001 (unpaired Student's *t*-test). n = 3-4 mice.

(K) Quantification of total vessel length in the MBH of LepR $^{i\Delta GFAP/+}$ mice chronically fed SC or HFHS diet as compared to littermate controls. Data are presented as mean ± SEM. *** P < 0.001, **** P < 0.0001 (unpaired Student's *t*-test). $^{\#}$ P < 0. 05 (one-way ANOVA). n = 3-4 mice.

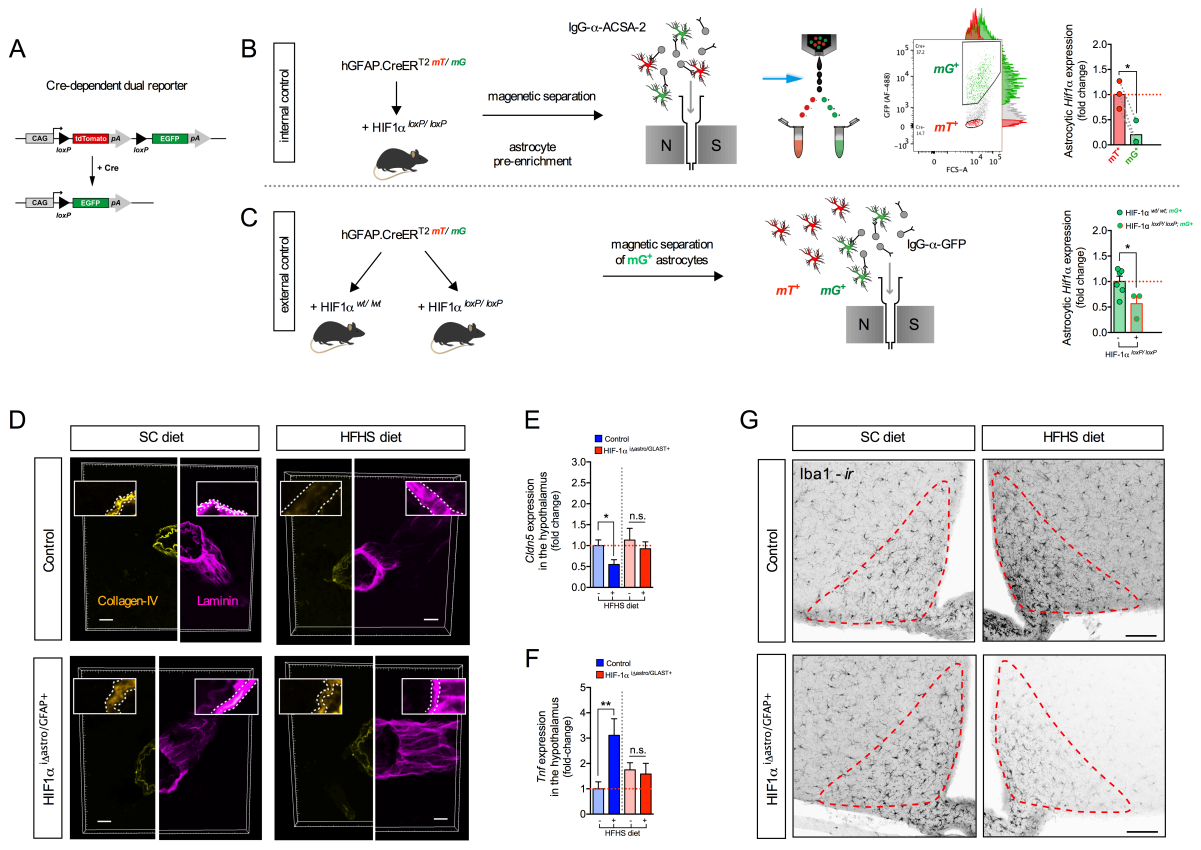

Figure S4. Related to Figure 4: Validation of downregulation of HIF-1α in GFAP-expressing astrocytes in HIF1α $^{AAV.Gfa2.iCre}$ mice and its extended cerebrovascular effects *in vivo*.

(A) Schematic diagram of the genomic organization of the a dual fluorescent Cre-dependent reporter mouse line ROSA $^{mT/mG}$ *(Gt(ROSA)26Sor* $^{tm4(ACTB-,tdTomato,-EGFP)/Luo}$ */J)*.

(B) Schematic depiction of the workflow used to pre-enrich astrocytes from tamoxifen-injected HIF1α $^{iΔGFAP\ mT/mG}$ mice using magnetic-assisted cell sorting using the marker astrocyte-specific antigen 2 (ACSA2). Non-recombined (Cre^-; mT^+; red) and recombined (Cre^+; mG^+; green) astrocytes were immediately separated using FACS; representative FACS plot with the x-axis representing FSC-A and the y-axis representing GFP / Alexa Fluor 488 fluorescence; gating of mG^+ (green) and mT^+ (red) populations is indicated by encirclements. qPCR analysis using exon 2 specific HIF1α probes indicating marked reduction of transcripts in recombined (green) astrocytes relative to non-recombined (red) astrocytes. Data are presented as mean ± SEM. * $P < 0.05$. n = 3 mice (unpaired Student's *t*-test).

(C) Schematic depiction of the workflow used to isolate recombined, mG^+ astrocytes from tamoxifen-injected HIF1α $^{iΔGFAP\ mT/mG}$ mice (HIF1α $^{loxP/loxP}$) and hGFAP.CreER $^{T2/mG+}$ reporter mice by magnetic-assisted cell sorting *via* anti-GFP directed antibodies (IgG-α -GFP); qPCR analysis using exon 2 specific HIF-1α probes of HIF1α $^{loxP/loxP}$ mice as compared to HIF1α $^{wt/wt}$ mice. Data are presented as mean ± SEM. * $P < 0.05$. n = 3-5 mice (unpaired Student's *t*-test).

(D) 3D-rendered confocal micrographs depicting HFHS-induced thickening of the vascular basement membrane as exemplified by collagen-IV (yellow) and laminin (magenta) in control littermates (upper panels) or HIF1α $^{i\Delta GFAP/+}$ (lower panels) mice either fed with a SC or a HFHS diet. Images are representative of data in **Figure 4E**. Scale bar, 10 µm.

(E) qPCR analysis of hypothalamic Claudin-5 (*Cldn5*) expression in HIF1α $^{i\Delta GLAST/+}$ mice and wildtype littermates either fed with a SC or a HFHS diet relative to SC diet-fed wildtypes. Data are presented as mean ± SEM. * $P < 0.05$, n.s., not significant. n = 6-11 mice (unpaired Student's *t*-test).

(F) qPCR analysis of hypothalamic Tumor-necrosis factor (*Tnf*) expression in HIF1α $^{i\Delta GLAST/+}$ mice and wildtype littermates either fed with a SC or a HFHS diet relative to SC diet-fed wildtypes. Data are presented as mean ± SEM. * $P < 0.05$, n.s., not significant. n = 6-11 mice (unpaired Student's *t*-test).

(G) Representative confocal micrographs illustrating the number of microglia immunoreactive for ionized calcium-binding adapter protein 1(Iba1-ir) in control and HIF1α $^{i\Delta GFAP/+}$ mice either fed with a SC or a HFHS diet. Images are representative of data in **Figure 4F**. Scale bar, 100 µm.

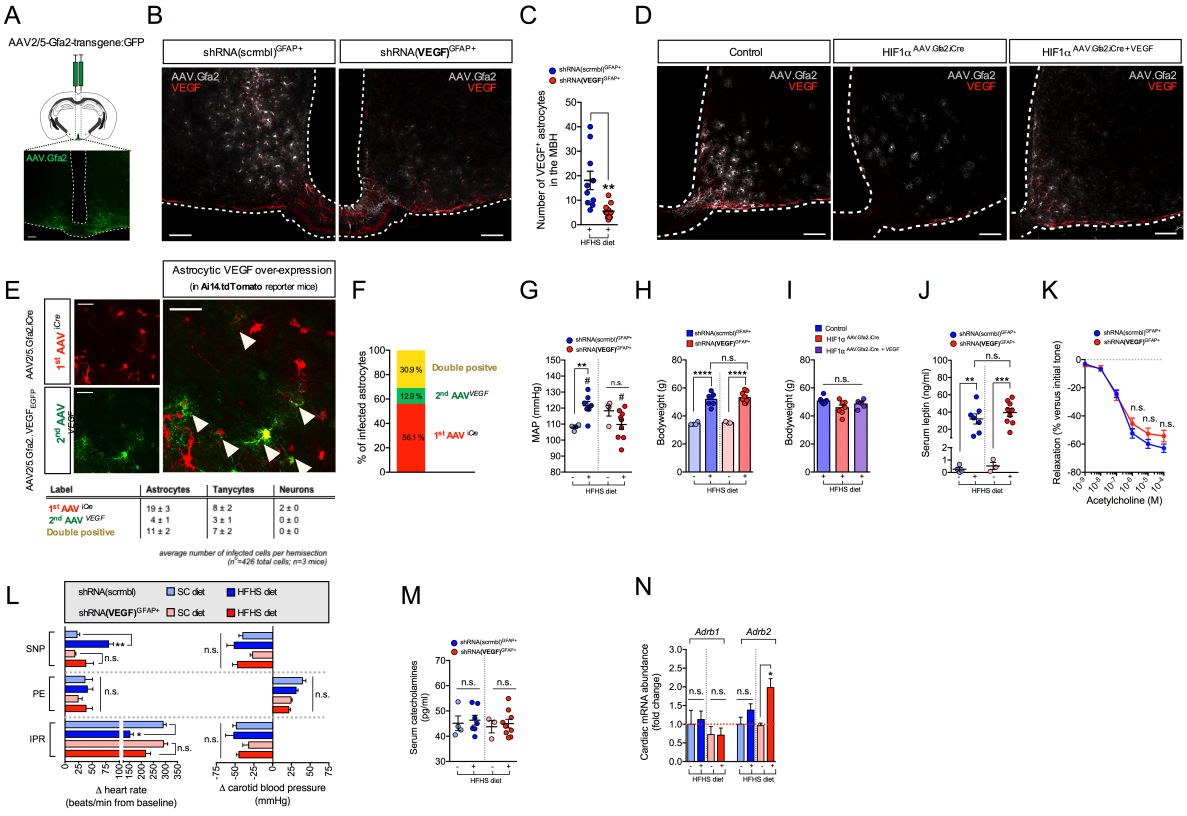

Figure S5. Related Figure 5: Cardiovascular and cardiometabolic alterations induced by astroglial VEGF knock-down.

(A) Schematic diagram of coronal brain section illustrating stereotaxic injections of AAV2/5 into the MBH of mice in order to drive transgene expression from the synthetic astrocyte-specific $Gfa2_{(2.2kb)}$ promoter. Representative confocal micrograph of AAV-targeted astrocytes within the MBH identified by viral GFP expression (AAV.Gfa2; green). Scale bar, 100 µm.

(B) Representative confocal micrographs of HFHS-diet fed shRNA(scrmbl)$^{GFAP+}$ and shRNA(VEGF)$^{GFAP+}$ mice showing VEGF immunoreactivity (red) along with virally expressed reporter protein (AAV.Gfa2; grey). Scans correspond to the same brain sections that are presented with regards to vascularity in **Figure 5B**. Scale bar, 100 µm.

(C) Corresponding quantification of VEGF-ir cells in the MBH. Data are presented as mean ± SEM. **p < 0.01. n = 3-5 mice (unpaired Student's *t*-test).

(D) Representative confocal micrographs of control mice as compared to HIF1α $^{AAV.Gfa2.iCre}$ and HIF1α $^{AAV.Gfa2.iCre + VEGF}$ mice showing VEGF immunoreactivity (red) along with virally expressed reporter protein (AAV.Gfa2; grey). Scans correspond to the same brain sections that are presented with regards to vascularity in **Figure 5D**. Scale bar, 100 µm.

(E) Characterization of dual virus approach in order to re-express VEGF in astrocytes otherwise devoid of HIF1α (HIF1α$^{AAV.Gfa2.iCre + VEGF}$ mice); both AAVs were mixed and simultaneously nanoinjected into the MBH of Cre-dependent Ai14.tdTomato reporter mice in order to visualize both Cre-recombined (red) as well as VEGF-overexpressing (green) cells; table below listing the absolute numbers of astrocyte, tanycytes and neurons per hemisection that were infected by either 1st AAV ^{iCre} (red) , 2nd AAV^{VEGF} (green) or both (yellow). n^0 = 426 cells. n = 3 mice. Scale bar, 25 µm.

(F) Percentage of all infected astrocytes either single or double-infected astrocytes targeted by either 1st AAV^{iCre} (red), 2nd AAV^{VEGF} (green) or both (yellow).

(G) Mean arterial pressure of shRNA(scrmbl)$^{GFAP+}$ and shRNA(VEGF)$^{GFAP+}$ mice fed either SC diet or HFHS diet as assessed by the tail cuff system assessed by repeated measures on separate days. Data are presented per individual mouse and mean ± SEM. ** P < 0.01. n.s., not significant. n = 3-7 mice (unpaired Student's *t*-test).

(H) Quantification of terminal bodyweights of shRNA(scrmbl)$^{GFAP+}$ and shRNA(VEGF)$^{GFAP+}$ mice fed either SC diet or HFHS diet. Data are presented per individual mouse and mean ± SEM. **** P < 0.0001. n = 3-7 mice (unpaired Student's *t*-test).

(I) Quantification of terminal bodyweights of HFHS diet fed control mice, HIF-1α $^{AAV.Gfa2.iCre}$ and HIF-1α $^{AAV.Gfa2.iCre+VEGF}$ mice. Data are presented per individual mouse and mean ± SEM. n.s., not significant. n = 7-8 mice (unpaired Student's *t*-test).

(J) Serum leptin levels of shRNA(scrmbl)$^{GFAP+}$ and shRNA(VEGF)$^{GFAP+}$ mice fed either SC diet or HFHS diet. Data are presented as mean ± SEM. ** P < 0.01, *** P < 0.001, n.s., not significant. n = 3-7 mice (unpaired Student's *t*-test).

(K) Quantification of dose-response curve of acetylcholine-induced endothelial relaxation of aortic ring segments of shRNA(scrmbl)^{GFAP} and shRNA(VEGF)$^{GFAP+}$ mice upon a HFHS diet feeding. Data is presented relative to initial tone and mean ± SEM. n.s., not significant. n = 6-7 mice (unpaired Student's *t*-test).

(L) Quantification of relative changes in heart rate as well as carotid artery pressure are displayed upon *intracarotid* administration of sodium nitroprusside (SNP; 500 µg/kg BW), phenylephrine (PE; 50 µg/kg BW) and isoproterenol (IPR; 50 µg/kg BW) in shRNA(scrmbl)$^{GFAP+}$ and shRNA(VEGF)$^{GFAP+}$ mice fed either SC diet or HFHS diet. Data are presented relative to baseline and mean ± SEM. * P < 0.05, ** P < 0.01n = 3-7 mice; 2-3 aortic ring segments/mouse (two-way ANOVA).

(M) Quantification of circulating catecholamines in serum of shRNA(scrmbl)$^{GFAP+}$ and shRNA(VEGF)$^{GFAP+}$ mice fed either SC diet or HFHS diet. Data are presented as mean ± SEM. n.s., not significant. n = 3-7 mice (unpaired Student's *t*-test).

(N) qPCR analysis of the cardiac expression of β_1-and β_2 adrenoreceptors (*Adrb1* and *Adrb2*, respectively) in shRNA(scrmbl)$^{GFAP+}$ and shRNA(VEGF)$^{GFAP+}$ mice fed either SC diet or HFHS diet. Data are presented as mean ± SEM. * P < 0.05, n.s., not significant. n = 3-7 mice (unpaired Student's *t*-test).